A possible evolutionary origin for the Mn_4 cluster of the photosynthetic water oxidation complex from natural MnO_2 precipitates in the early ocean

Kenneth Sauer*†‡ and Vittal K. Yachandra*‡

*Melvin Calvin Laboratory, Physical Biosciences Division, Lawrence Berkeley National Laboratory, and †Department of Chemistry, University of California, Berkeley, CA 94720

Communicated by Ignacio Tinoco, Jr., University of California, Berkeley, CA, May 3, 2002 (received for review March 14, 2002)

The photosynthetic water oxidation complex consists of a cluster of four Mn atoms bridged by O atoms, associated with Ca^{2+} and Cl^-, and incorporated into protein. The structure is similar in higher plants and algae, as well as in cyanobacteria of more ancient lineage, dating back more than 2.5 billion years ago on Earth. It has been proposed that the proto-enzyme derived from a component of a natural early marine manganese precipitate that contained a $CaMn_4O_9$ cluster. A variety of MnO_2 minerals are found in nature. Three major classes are spinels, sheet-like layered structures, and three-dimensional networks that contain parallel tunnels. These relatively open structures readily incorporate cations (Na^+, Li^+, Mg^{2+}, Ca^{2+}, Ba^{2+}, H^+, and even Mn^{2+}) and water. The minerals have different ratios of Mn(III) and Mn(IV) octahedrally coordinated to oxygens. Using x-ray spectroscopy we compare the chemical structures of Mn in the minerals with what is known about the arrangement in the water oxidation complex to define the parameters of a structural model for the photosynthetic catalytic site. This comparison provides for the structural model a set of candidate Mn_4 clusters—some previously proposed and considered and others entirely novel.

About 4.3 billion years ago (Ga) Earth was covered with an anoxic ocean (1). Although direct evidence is lacking before the beginning of the geological record about 3.8 Ga, there was almost certainly initially a level of dioxygen in the atmosphere that was vanishingly small (2, 3). The atmosphere comprised up to 10 bars of carbon dioxide (2) above a somewhat acidic ocean. Iron and manganese were introduced through high-temperature springs (>400°C). The ocean contained a large reservoir of reducing power in the form of Fe^{2+} and FeS (4–8). Short-wavelength UV radiation from a younger Sun drove the initial photochemical processes in the absence of a protective shield of dioxygen and ozone. Some of the iron and a small proportion of the manganese were photo-oxidized to mineral precipitates, such as ferric oxyhydroxide and birnessite [$(Na,Ca,K)(Mg,Mn)Mn_6O_{14}\cdot 5H_2O$], respectively (9, 10).

Whatever forms of life first appeared in this harsh environment are largely speculative (11, 12). Nevertheless, evidence of reduced carbon of biological origin is present from 3.8 Ga in crustal rocks (13, 14). In the presence of good reductants, such as sulfide, sulfur, dihydrogen, and prebiotic organic compounds, the precursors of microbial life as we know it on Earth somehow appeared. Methane, hydrogen, and bicarbonate nurtured the primitive organisms, with photo-produced ferric iron acting as the electron acceptor (8). Because light was an abundant but potentially powerful source of energy, biological organisms needed to find protection beneath minerals or through bioprecipitation to mitigate the effects of the far UV (15, 16). Photosynthesis began as an anoxygenic process, making use of light and reductants more powerful than water to fix CO_2 into organic carbon compounds (17–20). It is possible that precipitates or minerals such as FeS provided important catalytic surfaces for the biological redox reactions that were essential to these early photosynthetic organisms. Enzymes containing Fe_4S_4 clusters in a cubic lattice (ferredoxins) are ubiquitous in biology. Some multicentered iron-sulfur protein complexes serve as accumulators of electrons for reactions, such as those involved in the oxidation of dihydrogen, reduction of sulfate, and photosynthetic light reactions (21). It has been assumed that these clusters derived from the half-cell of the inverse spinel greigite (as $[Fe_4S_4][SFeS]_2$) in which the Fe and S appear in a cubic lattice (22).

As the available reductants, such as Fe^{2+}, dihydrogen, and sulfide/sulfur/thisulfate, gradually decreased or disappeared in local environments owing to photo-oxidation, water became the most available reductant for carbon fixation, and oxygenic photosynthesis as we know it today evolved. The accumulation of dioxygen in the atmosphere began about 2.5 Ga, although low concentrations date from about 3.4 Ga (23–25). One recent proposal invokes a thermodynamically favorable photo-transformation of bicarbonate to O_2 by a bacterial photosynthetic precursor during a period between anoxygenic photosynthesis and modern water-to-O_2 conversion (26).

A key component in the appearance of oxygenic photosynthesis was a complex that could store oxidizing equivalents to facilitate the four-electron oxidation of two water molecules to dioxygen, meanwhile making the electrons available for the reductive carbon-fixing reactions. We know that a four-atom manganese cluster serves the role of mediating water oxidation, leading to dioxygen formation in present-day photosynthesis (27). This is the case not only in higher plants and algae, which emerged relatively late in the geological record, but also in cyanobacteria, which represent our best example of the heritage of the earliest oxygenic photosynthetic organisms. As will be described presently, our knowledge of the structure and mechanism of the water oxidation enzyme makes it clear that the Mn_4 cluster is almost identical in higher plants and the descendents of primitive cyanobacteria (28, 29).

Blankenship and Hartman (30) have proposed an evolutionary path for oxygenic photosynthesis that involves hydrogen peroxide as an electron donor in a two-electron reaction to produce O_2. They suggest that the need to store only two oxidation equivalents would enable the electron transfer to be mediated by a two-Mn cluster, such as is found in the catalytic site of modern catalase enzymes. There seems to be no evidence, however, for the presence of significant H_2O_2 in the Archean environment. Furthermore, its conversion to O_2 and H_2O by dismutation is an exergonic reaction that does not require energy from light. Many compounds, such as MnO_2, that were certainly present in the Archean ocean serve as effective catalysts for the dismutation reaction.

Abbreviations: EXAFS, extended x-ray absorption fine structure; Ga, billion years ago; OEC, oxygen-evolving complex; PS II, photosystem II.

‡To whom reprint requests should be addressed. E-mail: khsauer@lbl.gov or vkyachandra@lbl.gov.

BIOPHYSICS

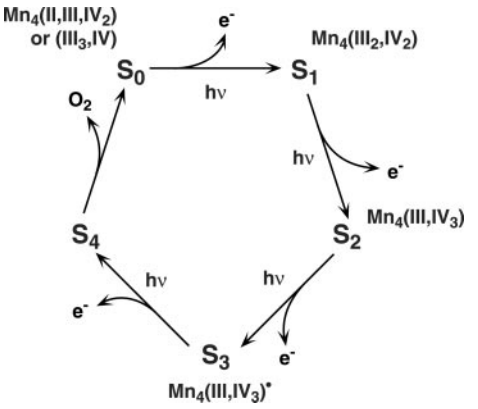

Fig. 1. The Kok cycle of S-state transitions in photosynthetic water oxidation. After four light-induced steps in which electrons are extracted by PS II, the metastable state S_4 is reached, which results in the release of O_2 within milliseconds. Proposed oxidation states of the four Mn atoms in each S-state are based on electron paramagnetic resonance and x-ray spectroscopic analysis.

The Photosynthetic Water Oxidation Enzyme

In the two-light reaction scheme of photosynthetic electron transport, water oxidation is associated with photosystem II (PS II). Manganese was recognized as an essential element for oxygenic photosynthesis more than 60 years ago (31). Subsequently, Ca^{2+} and Cl^- were also identified as required components (32–35). Depletion of these components from the growth medium or their removal from photosynthetic membranes (thylakoids) results in loss of the ability to evolve oxygen, although the light reactions themselves are not impaired.

Studies using single-turnover flashes showed that electrons are removed one at a time from the water oxidation complex in the four-electron transfer process (36); this observation led to the proposal by Bessel Kok of a cycle of four intermediate states (S-states) leading to O_2 evolution (37). The observation of a multiline electron paramagnetic resonance signal by Dismukes and Siderer (38) provided evidence that Mn plays a direct role in storing the oxidizing equivalents. Subsequent studies, especially those using electron paramagnetic resonance and x-ray absorption spectroscopy, have provided a basis for the scheme illustrated in Fig. 1. The successive absorption of photons by PS II results in a stepwise progress from the principal resting state, S_1, through the more oxidized S_2 and S_3 states, then to a hypothetical intermediate (S_4) that is precursor to the release of dioxygen together with the reduction of the complex to the S_0 state. The fourth photo-induced step returns the system to the S_1 state, and the cycle begins again. Spectroscopic evidence implicates redox reactions involving Mn in at least three of these four steps (39). In addition, the evidence supports the view that Mn cycles largely, although not necessarily exclusively, between the Mn(III) and Mn(IV) oxidation states.

PS II is a membrane-associated complex and is known to consist of a large assortment of proteins, pigment molecules, and bound cofactors (40). Two proteins, D1 and D2, which are the products of the *psbA* and *psbD* genes, constitute the matrix for the PS II reaction center, and D1 provides most of the binding sites for the Mn cluster. The determination of a high-resolution structure of PS II and the water oxidation complex is, as of this writing, incomplete. Preliminary announcement of an electron density map at 3.8-Å resolution identifies a ''pear-shaped'' region of electron density associated with the Mn_4 cluster (41).

Based primarily on extended x-ray absorption fine structure (EXAFS) analysis, we conclude that the Mn_4 cluster has the following attributes: it contains (*i*) at least two and probably three di-μ-oxo bridged Mn pairs, separated by 2.7–2.8 Å, (*ii*) one and possibly two mono-μ-oxo bridged Mn pairs, separated by approximately 3.3 Å, and (*iii*) at least one Mn-O-Ca link at approximately 3.4 Å (27). Furthermore, analysis of the EXAFS leads to the conclusion that the di-μ-oxo bridged Mn vectors are not colinear. The atoms immediately adjacent to the Mn in the cluster are thought to be largely oxygen, derived from protein backbone, amino acid side chains, water or oxo-bridges; one or two nitrogen atoms are also present (42–44). Although these properties provide limitations that are not as firm as we would like, they do appear to exclude a symmetric cubane-like Mn_4O_4 cluster, which was proposed by Brudvig and Crabtree (45), in the S-states that have been studied by EXAFS. The formation of a cubane in the elusive S_4 state (46–48) cannot be ruled out, however. Many topological tetranuclear Mn structures compatible with the observed EXAFS data have been presented (27, 28).

Manganese Oxide Minerals

In 2001 a proposal was put forth by M. J. Russell and A. J. Hall (University of Glasgow, Scotland) that manganese oxide precipitates may have provided the origin for the Mn_4 cluster of the water oxidation enzyme.[§] They proposed that a MnO_2-mineral like ranciéite ($CaMn_4O_9{\cdot}3H_2O$) was the source of the metal cluster, much along the lines that the Fe_4S_4 cubane was derived from an iron sulfide mineral, greigite (22). Russell and Hall speculated on how such a mineral-derived cluster may have provided the basis for the chemistry of the photosynthetic water oxidation reactions, based in part on model system investigations by Dismukes and coworkers (48, 49). These particular MnO_2 minerals are examples of layer-type or sandwich structures, as characterized in an excellent review by Post (50). They occur widely in seafloor manganese-iron nodules, submarine exhalites, soils, rock varnishes, and minerals that have been exposed to weathering in the atmosphere (51). On the basis of an analysis of x-ray powder-diffraction patterns of these minerals and synthetic analogs, the deduced structures of the large layer-type family consist of alternating two-dimensional lattices of MnO_2, with interlayer sites containing cations (Ca^{2+} in the case of ranciéite) and water (Fig. 2). The spacing layers contain important components of the water oxidation reaction and may be envisioned to provide for the ready exchange, at least near the mineral surface, of those components with a surrounding aqueous matrix. The MnO_2 layer is typically imperfect, in the sense that occasional Mn atom sites are vacant, probably on a random basis, and the exchangeable cations are bound in the spacing layers above and below the vacant sites (see Fig. 2*b*) (52). In some minerals there is a significant amount of Mn(III) along with the predominant Mn(IV), providing additional locations for charge-balancing cations (50). It is apparent that Mn_4 clusters, along with the associated O ligands and cations, could have contributed either directly to mineral growth or as the ''ready-made'' prerequisites for a nascent water oxidation complex. We find this to be an appealing hypothesis that merits further investigation.

Measured against the criteria listed above that provide a spectroscopic characterization of the modern water oxidation complex, however, the layer-type minerals exhibit notable differences. The birnessite/ranciéite MnO_2 lattice does not exhibit any of the intermediate 3.3- to 3.4-Å Mn-Mn vectors (referred to as the 3.4-Å vector hereafter) characteristic of mono-μ-oxo bridged Mn units and that are seen in the photosynthetic complex. Only short 2.7- to 2.8-Å vectors (referred to as the 2.8-Å vector hereafter) characteristic of the di-μ-oxo bridged Mn units and those significantly longer, at least 5 Å, are present (Fig.

[§]Russell, M. J. & Hall, A. J., Sixth International Congress on Carbon Dioxide Utilization, Sept. 9–14, 2001, Breckenridge, CO, abstr., p. 49.

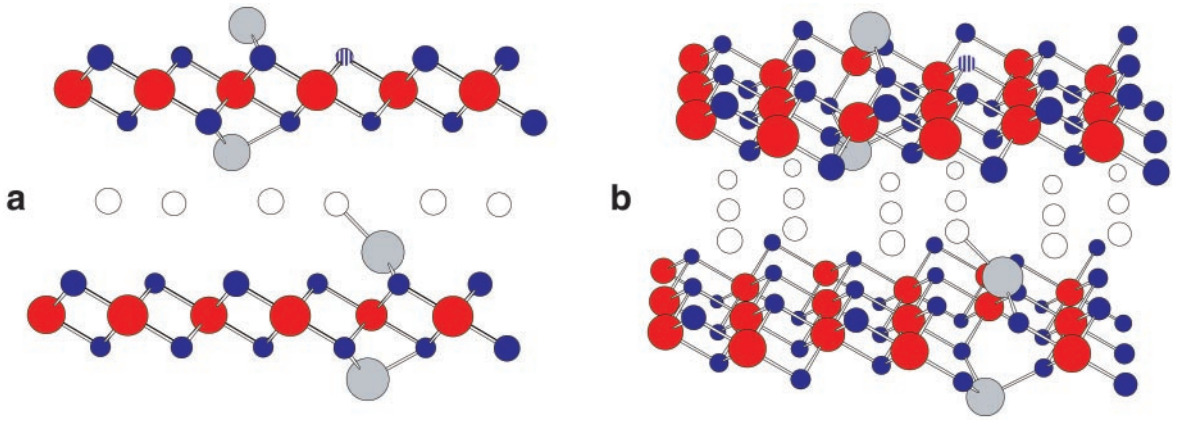

Fig. 2. (*a*) End-on view of the birnessite lattice (layer type) consisting of Mn (red) and O (blue) atoms. There is only one kind of bridging O atom (sp^3-like between the Mn atoms; one of them is shown in vertical stripes). Mg^{2+} cations (gray) are located between the manganese and oxygen layers. The water molecules between the layers are shown as ○. (*b*) Oblique view of the lattice showing the mode of apical bridging of the O atoms among three Mn atoms.

2). The 3.4-Å distances are, however, present in the tunnel-type minerals (Fig. 3) (50, 53). To appreciate the structural distinctions that are involved here, it is significant to note that all of the Mn atoms are octahedrally coordinated to O atoms in the idealized structures of the three principal classes of MnO_2 minerals: spinels, layer type, and tunnel type. The bonding of the O atoms, on the other hand, falls into two categories: sp^3-like, providing for an apical position of the O with respect to the three associated Mn atoms, and sp^2-like, where the bonded O atom is in the same plane as the three Mn. The spinels and the MnO_2 lattices in the layer-type minerals contain only sp^3-like oxygens (Fig. 2). As a consequence, no intermediate 3.4-Å Mn-Mn vectors are present in these lattices. In the tunnel-type minerals, however, there are also sp^2-like oxygens present; the occurrence of 3.4-Å vectors in these lattices is a direct consequence of the presence of the sp^2-like oxygens (Fig. 3).

Tunnel-type Mn oxide minerals are found around submarine hot springs (51, 54, 55) and are also widespread in soils and weathered rocks. They consist of three-dimensional lattices of Mn and O atoms in the approximate ratio 1:2. The lattice structures are typically penetrated by parallel tunnels that occur with different cross-sectional dimensions, depending on the particular mineral (50). In the idealized lattices, the tunnels are of infinite length. The tunnel dimensions have been designated 1×1 (pyrolusite), 1×2 (ramsdellite), 2×2 (hollandite), 2×3 (romanèchite), and 3×3 (todorokite) (50, 51). One report describes a synthetic analog with 2×5 tunnels (56). Pyrolusite, which has the smallest tunnels, has only sp^2-like O atoms in its lattice. The pyrolusite lattice is rich in 3.4-Å Mn-Mn vectors—four times as many as 2.8-Å vectors. EXAFS studies of several of these minerals show a good correlation between the relative scattering amplitudes and the vector ratios for the known structures (53). The minerals with larger tunnels contain a mix of sp^3- and sp^2-like oxygens. The lattices contain both 2.8- and 3.4-Å Mn-Mn vectors, with relative populations typically in the range 1:1 to 3:2. These lattices are complex, however, giving rise to a large assortment of configurations involving bonded clusters of four Mn atoms.

The tunnels in pyrolusite and ramsdellite are too small to accommodate cations or more than a minimal amount of water (50). These minerals have the stoichiometric composition MnO_2. However, beginning with hollandite (2×2 tunnels) and extending to the minerals with larger tunnels, the dimensions are sufficient to accommodate water and cations in the tunnels. The variety of cations found in nature is quite large, including monovalent ions such as Li^+, Na^+, K^+, and H^+, divalent ions Mg^{2+}, Ca^{2+}, Ba^{2+}, Mn^{2+}, and even trivalent ions (Fig. 3 *a* and *b*). The synthetic lattice with 2×5 tunnels contains Rb^+ ions, which are quite large (56). Furthermore, the tunnels are large enough that water and the ions are able to diffuse in and out, at least on the geological time scale. The large variations in chemical composition of the minerals doubtless reflects the nature of the aqueous/ionic/thermal environmental history of the deposit from which they were obtained. Synthetic analogs of the tunnel-type minerals with better-defined composition can be made by thermochemical methods.

Analysis of the internal structures of these minerals using x-ray crystallography shows that the locations of cations or water typically exhibit partial occupancy. This is a consequence of the inherent disorder present in the lattices of the larger tunnel-type minerals. Sizable single crystals of these minerals are difficult to find; several of the structures are determined or inferred on the basis of the analysis of powder diffraction measurements and by analogy to similar structures with better definition. However, single crystal diffraction of hollandite (57) and a synthetic analog (58) have been reported. The disorder, together with the presence of cations, also reflects the presence of Mn oxidation states other than Mn(IV). In particular, the occurrence of Mn(III) at a (presumably random) site in the lattice is associated with significant distortion of the octahedral coordination geometry, owing to the Jahn–Teller effect of Mn(III) (50). It should be noted in passing that these irregularities or sites of disorder provide for a potentially rich source of possible chemical interactions with ions, water, or other molecules in the vicinity. Much of this "catalytic" chemistry presumably occurs at surface sites of these microcrystalline materials.

Although modeling even idealized lattices of the family of tunnel-type MnO_2 minerals gives rise to a bewildering array of structures, nevertheless the components of these structures are quite regular and relatively few in number. Briefly, considering the tunnels to be approximately square or rectangular in cross section, the local clustering of Mn and O falls into two categories: clusters associated with tunnel corners and those associated with lengthening sides. The corner clusters in all lattices with large tunnels are identical; they contain both sp^2- and sp^3-like O atom links. The side-lengthening components, by contrast, contain only sp^3-like O atom links (see Fig. 3). In fact, they consist entirely of networks like the MnO_2 lattice in the layer-type structures. Thus, the lattice of idealized hollandite with 2×2 tunnels contains all of the possible four-Mn cluster arrangements that are present in the minerals with larger tunnels. Despite the fact that, as we have discovered, there are more than 30 such

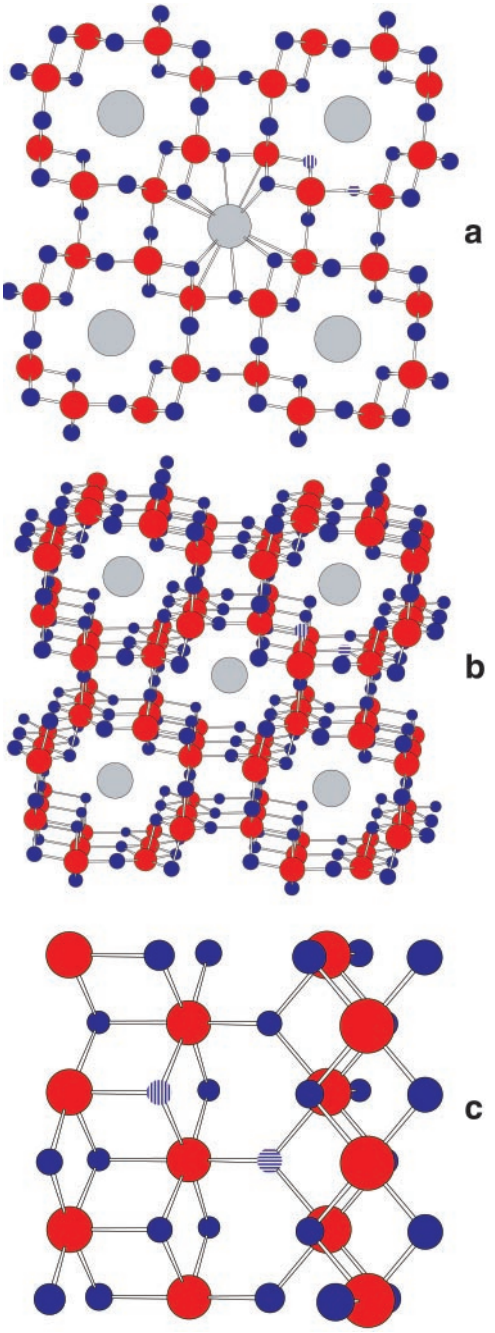

Fig. 3. (*a*) End-on view of the hollandite lattice (tunnel type) consisting of Mn (red) and O (blue) atoms and showing the proposed location of Ba^{2+} cations (gray) in the 2 × 2 tunnels (57, 58). There are two kinds of bridging O atoms, and one of each kind is designated by vertical stripes (sp^3-like) or horizontal stripes (sp^2-like). (*b*) Oblique view of the hollandite lattice shows the difference in the mode of bridging of the sp^3-like (apical) and sp^2-like (planar) O atoms between three Mn atoms. (*c*) Expanded oblique view shows more clearly the differences between the sp^3-like (vertical stripes) and sp^2-like (horizontal stripes) bridging O atoms.

topologically distinct Mn_4 cluster arrangements in hollandite, it is sufficient to analyze the situation in this one representative mineral to extract an essentially complete set of such geometric arrangements present in the entire class of tunnel-type minerals. At the same time, we need to be aware that imperfections in the lattices, especially the presence of Mn(III), and surface sites greatly expand the possibilities.

Mn_4 Clusters in the Minerals

We used a computer-generated model to extract clusters of four Mn atoms joined contiguously by O-links from the hollandite lattice, with coordinates derived from the x-ray crystallographic data. This process yields an assortment of putative clusters that provides candidates for a potentially catalytic site. In our effort to do this, we did not try to maintain links to divalent cations, which are in any case mobile and ill defined in the electron density maps. To organize the extracted possible four-Mn cluster types, we categorize the Mn-Mn distances in terms of the number of 2.8-Å vectors, **A**, and the number of 3.4-Å vectors, **B**, per four Mn, as (**A, B**). Thus, a cubic Mn_4O_4 cluster, which actually does not occur as such in any of the layer-type or tunnel-type lattices, is in category (**6, 0**). Fig. 4*a* includes categories (**5, 0**) (**4, 1**), (**3, 0**), (**2, 3**), (**1, 4**), (**1, 3**), and (**1, 2**) that are not compatible with that present in the oxygen-evolving complex (OEC). Structures of some of the more interesting clusters that conform to the categories (**3, 2**) (**3, 1**), (**2, 2**), and (**2, 1**) that can be present in the OEC are shown in Fig. 4*b*. We have included only clusters that are topologically distinct, in the sense that chemical bonds need to be broken and/or formed to convert any one of them into another. Also, we do not include mirror-image clusters or clusters than can be generated by rotation about a bond. Many of the clusters would be expected to be flexible once they are extracted; for example, where a Mn atom is joined to the rest of the cluster by a mono-μ-oxo link. In other cases the arrangement of the atoms in the cluster should be rigid. Especially where the possibility of flexibility is present, the incorporation of the cluster core into a protein binding site would be expected to conform it to a particular geometry. Both bridging and terminal ligand exchange (59–62) and cluster reorganization (63, 64) is known to occur in inorganic Mn complexes, and this process could provide an avenue for the incorporation of the Mn clusters from the precipitates into a peptide. This would provide a method of fine tuning to optimize catalytic activity, modify energy requirements involved in oxidation-state changes, and facilitate the incorporation of water and the formation of the O—O bond leading to dioxygen. The essential divalent cation Ca^{2+} and possibly the Cl^- anion could also be incorporated into the protoenzyme in a way that parallels their incorporation into the mineral, again subject to subsequent rearrangement by evolution to optimize function.

On the basis of the structural criteria established for the modern photosynthetic water oxidation enzyme with spectroscopic methods, we favor candidate structures in categories (**3, 2**) and (**3, 1**) over those in (**2, 2**) or (**2, 1**), but any of these may be considered to be "acceptable," given the limits on the stringency of the criteria. We disfavor those clusters with only a single 2.8-Å Mn-Mn vector or with no 3.4-Å vectors. Furthermore, we feel that the experimental evidence provides strong evidence against the presence of two or more colinear and contiguous 2.8-Å vectors. This still leaves many Mn_4 clusters in the acceptable class. Some of these may be judged more likely than others on the basis of providing a sufficiently pear-shaped electron density distribution; however, that criterion will be easier to apply once a higher-resolution map is available.

Other criteria may prove useful to narrow the range of possibilities. We have shown, for example, that it is possible to measure polarized EXAFS on oriented thylakoid membranes and to record EXAFS dichroism as a function of the orientation of the membrane normal relative to the x-ray electric vector (65). This approach provides limitations on the possible angles between vectors within the water oxidation cluster. Each of the rigid-cluster candidates can be examined against these measurements, and even those clusters with limited flexibility may prove susceptible to exclusion or inclusion on this basis. The possibility of making polarized measurements on single crystals of PS II

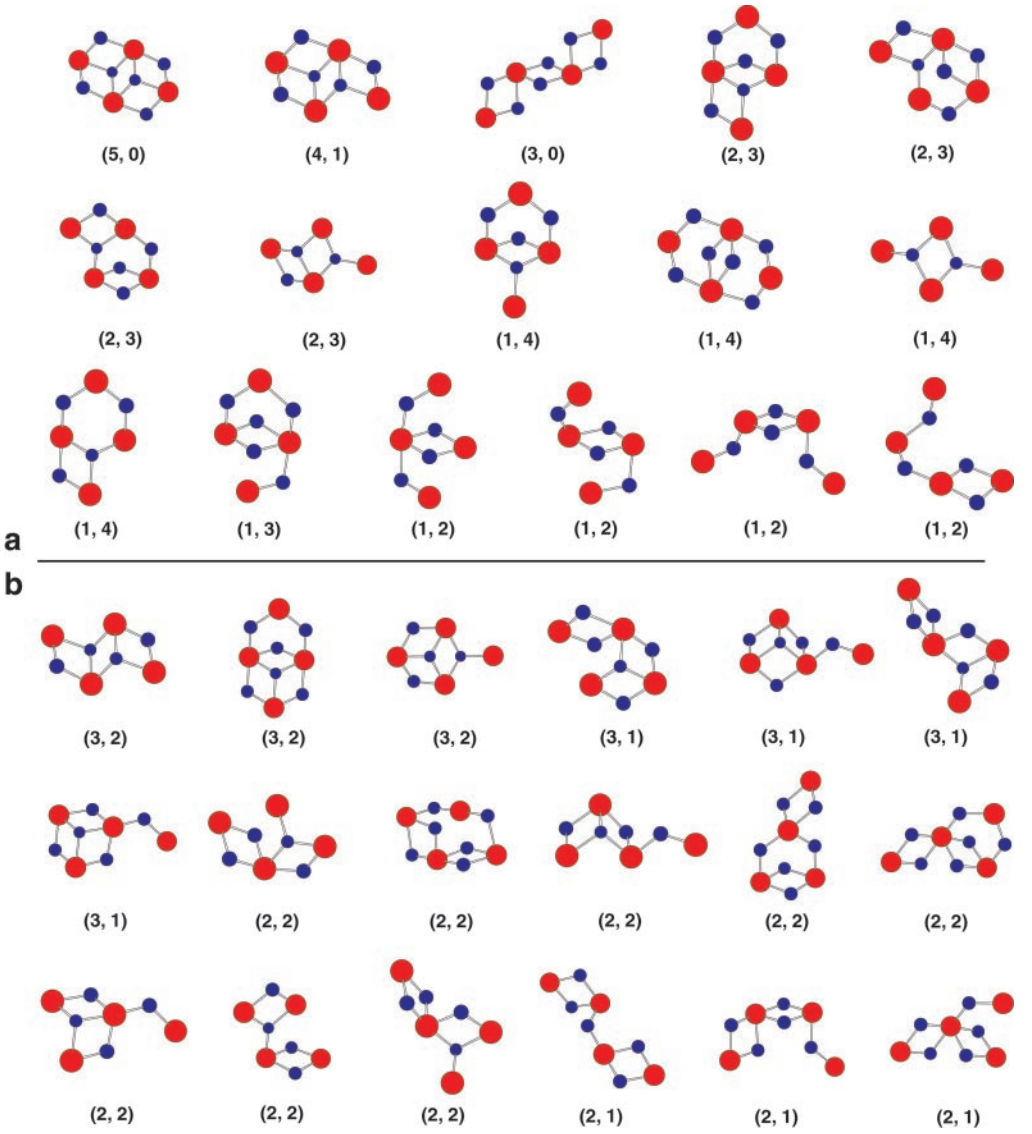

Fig. 4. Some possible Mn_4 clusters and oxygens extracted from the hollandite lattice (*a*) in categories that are incompatible with that present in the OEC, and (*b*) those that are compatible with that associated with the OEC. Structures are organized according to **A**, the number of 2.8-Å Mn-Mn vectors, and **B**, the number of 3.4-Å vectors, and given the designation (**A**, **B**). Only the bridging O atoms are shown.

provides an even richer opportunity, and we hope to pursue such measurements in the near future.

Conclusion

The hypothesis of Russell and Hall that the origin of the photosynthetic water oxidation complex may be reflected in the structure of manganese minerals[§] provides an intriguing adjunct to the growing picture of how life on Earth evolved. We know that the photosynthetic water oxidation complex is not formed by direct incorporation of such a preformed cluster in present-day organisms. The evolution of the modern complex, however, presumably began in the absence of the refined PS II protein binding site and fully developed mechanism for photo-oxidizing Mn^{2+} during its incorporation. It is well known that solid MnO_2 exhibits pronounced "catalase" activity in its ability to increase the rate of decomposition of H_2O_2 into H_2O and O_2 by many orders of magnitude. A primitive organism that succeeded in the task of oxidizing water to H_2O_2 could then make use of a $CaMn_4$ cluster to complete the conversion to O_2. There is no evidence that free H_2O_2 is produced by PS II in present-day photosynthesis, but a bound peroxide link in one of the intermediate S-states is a possibility. It is also possible that the further conversion of H_2O_2 to O_2 was especially valuable in a symbiotic relation with another primitive organism that depended on respiration. The hypothesis has also considerably enlarged our repertoire of possible Mn_4 clusters. We will benefit from these ideas during the interval of uncertainty until a high-resolution structure of the water oxidation complex is available.

We particularly express our appreciation to Profs. Michael Russell (Univ. of Glasgow) and Robert Blankenship (Arizona State Univ.) for their careful reading of the manuscript and excellent suggestions for its improvement. We have also benefited from discussions with Prof. Gary Brudvig (Yale Univ.), Prof. G. Charles Dismukes (Princeton Univ.), Dr. Peter Sauer (Indiana Univ.), and Prof. Jeffrey Long (Univ. of California, Berkeley). Eric Tulsky was most helpful in locating sources of crystallographic data for the mineral structures. We thank Dr. Heinz Frei (Lawrence Berkeley National Laboratory) for bringing this topic to our

attention and Drs. Roehl Cinco, Henk Visser, Junko Yano, and Uwe Bergmann at the Lawrence Berkeley National Laboratory for helpful discussions. This research was supported by National Institutes of Health Grant GM-55302 and the Director, Office of Science, Office of Basic Energy Sciences, Division of Energy Biosciences of the U.S. Department of Energy under Contract DE-AC03-76SF00098.

1. Lowe, D. R. (1994) in *Early Life on Earth*, *Nobel Symposium No. 84*, ed. Bengtson, S. (Columbia Univ. Press, New York), pp. 24–35.
2. Kasting, J. F. (1993) *Science* **259,** 920–926.
3. Towe, K. M. (1994) in *Early Life on Earth, Nobel Symposium No. 84*, ed. Bengtson, S. (Columbia Univ. Press, New York), pp. 36–47.
4. Chang, S. (1994) in *Early Life on Earth*, *Nobel Symposium No. 84*, ed. Bengtson, S. (Columbia Univ. Press, New York), pp. 10–23.
5. Schopf, J. W. & Klein, C., eds. (1992) *The Proterozoic Biosphere* (Cambridge Univ. Press, Cambridge, U.K.).
6. Appel, P. W. U., Rollinson, H. R. & Touret, J. L. R. (2001) *Precambrian Res.* **112,** 27–49.
7. Walker, J. C. G. & Brimblecombe, P. (1985) *Precambrian Res.* **28,** 205–222.
8. Russell, M. J. & Hall, A. J. (1997) *J. Geol. Soc. (London)* **154,** 377–402.
9. Braterman, P. S., Cairns-Smith, A. G. & Sloper, R. W. (1983) *Nature (London)* **303,** 163–164.
10. Anbar, A. D. & Holland, H. D. (1992) *Geochim. Cosmochim. Acta* **56,** 2595–2603.
11. Schopf, J. W. (1993) *Science* **260,** 640–646.
12. Schopf, J. W. (1999) *Cradle of Life* (Princeton Univ. Press, Princeton).
13. Schidlowski, M. (1988) *Nature (London)* **333,** 313–318.
14. Rosing, M. T. (1999) *Science* **283,** 674–676.
15. Pierson, B. K., Mitchell, H. K. & Ruff-Roberts, A. L. (1993) *Orig. Life Evol. Biosphere* **23,** 243–260.
16. Phoenix, V. R., Konhauser, K. O., Adams, D. G. & Bottrell, S. H. (2001) *Geology* **29,** 823–826.
17. Schopf, J. W., ed. (1983) *Earth's Earliest Biosphere* (Princeton Univ. Press, Princeton).
18. Xiang, J., Fischer, W. M., Inoue, K., Nakahara, M. & Bauer, C. E. (2000) *Science* **289,** 1724–1730.
19. Blankenship, R. E. (2002) *Molecular Mechanisms of Photosynthesis* (Blackwell, Oxford), pp. 220–243.
20. Olson, J. M. (2001) *Photosynth. Res.* **68,** 95–112.
21. Schoepp, B., Brugna, M., Lebrun, E. & Nitschke, W. (1999) in *Advances in Inorganic Chemistry: Iron-Sulfur Proteins*, eds. Sykes, A. G. & Cammack, R. (Academic, San Diego), pp. 335–360.
22. Russell, M. J., Daniel, R. M., Hall, A. J. & Sherringham, J. A. (1994) *J. Mol. Evol.* **39,** 231–243.
23. Des Marais, D. J., Strauss, H., Summons, R. E. & Hayes, J. M. (1992) *Nature (London)* **359,** 605–609.
24. Canfield, D. E., Habicht, K. S. & Thamdrup, B. (2000) *Science* **288,** 658–661.
25. Farquhar, J., Bao, H. & Thiemens, M. (2000) *Science* **289,** 756–758.
26. Dismukes, G. C., Klimov, V. V., Baranov, S. V., Kozlov, Y. N., DasGupta, J. & Tyryshkin, A. (2001) *Proc. Natl. Acad. Sci. USA* **98,** 2170–2175.
27. Yachandra, V. K., Sauer K. & Klein, M. P. (1996) *Chem. Rev.* **96,** 2927–2950.
28. DeRose, V. J., Mukerji, I., Latimer, M. J., Yachandra, V. K., Sauer, K. & Klein, M. P. (1994) *J. Am. Chem. Soc.* **116,** 5239–5249.
29. McDermott, A. E., Yachandra, V. K., Guiles, R. D., Cole, J. L., Britt, R. D., Dexheimer, S. L., Sauer, K. & Klein, M. P. (1988) *Biochemistry* **27,** 4021–4031.
30. Blankenship, R. E. & Hartman, H. (1998) *Trends Biochem. Sci.* **23,** 94–97.
31. Pirson, A. (1937) *Z. Bot.* **31,** 193–267.
32. Ghanotakis, D. F., Babcock, G. T. & Yocum, C. F. (1984) *FEBS Lett.* **167,** 127–130.
33. Yocum, C. F. (1991) *Biochim. Biophys. Acta* **1059,** 1–15.
34. Homann, P. H. (1987) *J. Bioenerget. Biomembr.* **19,** 105–123.
35. Coleman, W. J. (1990) *Photosynth. Res.* **23,** 1–27.
36. Joliot, P., Barbieri, G. & Chabaud, R. (1969) *Photochem. Photobiol.* **10,** 309–329.
37. Kok, B., Forbush, B. & McGloin, M. (1970) *Photochem. Photobiol.* **11,** 457–475.
38. Dismukes, G. C. & Siderer, Y. (1981) *Proc. Natl. Acad. Sci. USA* **78,** 274–278.
39. Messinger, J., Robblee, J. H., Bergmann, U., Fernandez, C., Glatzel, P., Visser, H., Cinco, R. M., McFarlane, K. L., Bellacchio, E., Pizarro, S. A., *et al*. (2001) *J. Am. Chem. Soc.* **123,** 7804–7820.
40. Debus, R. J. (1992) *Biochim. Biophys. Acta* **1102,** 269–352.
41. Zouni, A., Witt, H. T., Kern, J., Fromme, P., Krauss, N., Saenger, W. & Orth, P. (2001) *Nature (London)* **409,** 739–743.
42. DeRose, V. J., Yachandra, V. K., McDermott, A. E., Britt, R. D., Sauer, K. & Klein, M. P. (1991) *Biochemistry* **30,** 1335–1341.
43. Debus, R. J. (2000) in *Manganese and Its Role in Biological Processes*, eds. Sigel, A. & Sigel, H. (Dekker, New York), pp. 657–711.
44. Tang, X. S., Diner, B. A., Larsen, B. S., Gilchrist, M. L., Lorigan, G. A. & Britt, R. D. (1994) *Proc. Natl. Acad. Sci. USA* **91**, 704–708.
45. Brudvig, G. W. & Crabtree, R. H. (1986) *Proc. Natl. Acad. Sci. USA* **83,** 4586–4588.
46. Christou, G. & Vincent, J. B. (1987) *Biochim. Biophys. Acta* **895,** 259–274.
47. Ruettinger, W. F., Campana, C. & Dismukes, G. C. (1997) *J. Am. Chem. Soc.* **119,** 6670–6671.
48. Yagi, M., Wolf, K. V., Baesjou, P. J., Bernasek, S. L. & Dismukes, G. C. (2001) *Angew. Chem. Int. Ed. Engl.* **40,** 2925–2928.
49. Ruettinger, W., Yagi, M., Wolf, K., Bernasek, S. & Dismukes, G. C. (2000) *J. Am. Chem. Soc.* **122,** 10353–10357.
50. Post, J. E. (1999) *Proc. Natl. Acad. Sci. USA* **96,** 3447–3454.
51. Burns, R. G. & Burns, V. M. (1979) in *Marine Minerals: Reviews in Mineralogy*, ed. Burns, R. G. (Mineralogical Soc. Am., Washington, DC), Vol. 6, pp. 1–46.
52. Post, J. E. & Veblen, D. R. (1990) *Am. Mineral.* **75,** 477–489.
53. McKeown, D. A. & Post, J. E. (2001) *Am. Mineral.* **86,** 701–713.
54. Cornell, D. H. & Schütte, S. S. (1995) *Mineral. Deposita* **30,** 146–151.
55. De Villiers, J. E. (1983) *Econ. Geol.* **78,** 1108–1118.
56. Tamada, O. & Yamamoto, N. (1986) *Mineral. J.* **13,** 130–140.
57. Miura, H. (1986) *Mineral. J.* **13,** 119–129.
58. Vicat, J., Fanchon, E., Strobel, P. & Qui, D. T. (1986) *Acta Crystallogr. B* **42,** 162–167.
59. Wemple, M. W., Tsai, H.-L., Folting, K., Hendrickson, D. N. & Christou, G. (1993) *Inorg. Chem.* **32,** 2025–2031.
60. Wemple, M. W., Adams, D. M., Hagen, K. S., Folting, K., Hendrickson, D. N. & Christou, G. (1995) *J. Chem. Soc. Commun.*, 1591–1593.
61. Wemple, M. W., Adams, D. M., Folting, K., Hendrickson, D. N. & Christou, G. (1995) *J. Am. Chem. Soc.* **117,** 7275–7276.
62. Wang, S., Tsai, H.-L., Libby, E., Folting, K., Streib, W. E., Hendrickson, D. N. & Christou, G. (1996) *Inorg. Chem.* **35,** 7578–7589.
63. Wang, S., Folting, K., Streib, W. E., Schmitt, E. A., McCusker, J. K., Hendrickson, D. N. & Christou, G. (1991) *Angew. Chem. Int. Ed. Engl.* **30,** 305–306.
64. Wang, S., Tsai, H.-L., Hagen, K. S., Hendrickson, D. N. & Christou, G. (1994) *J. Am. Chem. Soc.* **116,** 8376–8377.
65. Mukerji, I., Andrews, J. C., DeRose, V. J., Latimer, M. J., Yachandra, V. K., Sauer, K. & Klein, M. P. (1994) *Biochemistry* **33,** 9712–9721.